Desalination and Water Treatment
www.deswater.com
doi: 10.1080/19443994.2016.1138896

57 (2016) 24456–24466
November

Taylor & Francis
Taylor & Francis Group

Synthesis of CuS nanoparticles and evaluation of its antimicrobial properties in combination with *Linum usitatissimum* root and shoot extract

M. Ghaedi[a,*], M. Yousefi-Nejad[b], M. Safarpoor[a], H.Z. Khafri[a], Inderjeet Tyagi[c], Shilpi Agarwal[d], Vinod Kumar Gupta[c,d,*]

[a]*Department of Chemistry, Yasouj University, Yasouj 75918-74831, Iran, Tel. +91 7432223048; emails: m_ghaedi@yu.ac.ir (M. Ghaedi), safarpoormohamad@yahoo.com (M. Safarpoor), khafri.zare@yahoo.com (H.Z. Khafri)*
[b]*Department of Biology, Yasouj University, Yasouj, 75918-74831, Iran, email: yousefi88@gmail.com*
[c]*Department of Chemistry, Indian Institute of Technology, Roorkee 247667, India, Tel. +91 1332 285801; email: indertyagi011@gmail.com (I. Tyagi), Tel. +91 1332285801, +91 1332 285043; Fax: +91 1332273560; emails: vinodfcy@iitr.ac.in, vinodfcy@gmail.com (V.K. Gupta)*
[d]*Department of Applied Chemistry, University of Johannesburg, Johannesburg, South Africa, email: shilpi.agarwal2307@gmail.com (S. Agarwal)*

Received 29 September 2015; Accepted 2 January 2016

ABSTRACT

Hydroalcoholic extracts have been prepared from *Linum usitatissimum* with maceration method, which was later examined for its antimicrobial activity in the presence of CuS nanoparticles by broth macrodilution and agar disc diffusion, and the determination of minimal inhibitory concentration of antibacterial agent required to inhibit growth of a pathogen, i.e. minimal inhibitory concentration and the lowest concentration of an antibacterial agent required to kill a particular bacterium, i.e. minimal bactericidal concentration were well elucidated and evaluated for these materials. The superposition of metal nanoparticles with the *L. usitatissimum* extracts was found to be effective in the eradication of the bacterial infections, and proved to be a good alternative of antibiotics. Antioxidant content of the extracts was also determined and demonstrated the highest antioxidant activities associated with the shoot of *L. usitatissimum* (Total phenolic content 1: 128.24 ± 1.127-mg gallic acid equivalents/g of dried extract, DPPH: 30.57 ± 0.4% inhibition, Ferric reducing antioxidant power: 957.8 ± 3.81 μmol Fe(II)/mg of dried extract and Total Flavonoid Content: 2: 95.04 ± 0.53-mg rutin equivalents (RuE)/g of dried extract).

Keywords: CuS nanoparticles; Antioxidant; Antibacterial; Antimicrobial; Extracts

1. Introduction

Plants have been used as a source of medicine from ages and today scientists recognize their value as a source of new medicinal product or complimentary to currently developed medicinal products [1] for the augmentation purpose. The plant-based medicine system plays an essential role in the health care as it is estimated that about 80% of population was relaying on traditional medicines as a primary health care [2]. Nanotechnology is an interdisciplinary area of science which has been burgeoning interest across the globe with huge momentum to usher in forming

*Corresponding authors.

nano-revolution. An important area in nanotechnology deals with the synthesis of nanoparticles which has encountered immense progress due to innumerable applications in recent decades [3]. Nanoparticles are particles less than 100 nm in diameter that exhibit new and enhanced size-dependent properties compared to its bulk material [4]. Metal nanoparticles have been instrumental as these exhibit completely new or improved properties compared with larger particles of the bulk materials, and these novel properties are derived due to the variation in specific characteristics such as size, distribution, and morphology of the particles. Nanoparticles possess a higher surface area to volume ratio with decrease in the size of the particles. Specific surface area is relevant to catalytic activity and other related properties [5–7].

Copper-based nanomaterials are used in a range of established and emerging technologies that include catalysts, printable electronics, magnetic storage, solar energy conversion, wood protection, and antimicrobial products [8–14]. Human beings have been using copper (Cu) and Cu complexes for various purposes for centuries, such as water purifiers, algaecides, fungicides, and as antibacterial and antifouling agents [15]. CuS nanoparticles have several advantages such as the low cost, simple and easy preparation, and small size for targeting [16]. Several researchers synthesize nanoparticles that posses the antimicrobial properties also [17–40], but none of them combined it with plant extracts.

The present study was focused on the synthesis and characterization of CuS nanoparticles. Later on, the enhancement of CuS nanoparticles by plant extract of *L. usitatissimum* (CuS/extract) as an antimicrobial agent and as antibiotic in the modern treatment was well elucidated and investigated.

2. Experimental

2.1. Materials and methods

All chemicals including copper acetate, zinc acetate, thioacetamide, tri-sodium citrate, Mueller Hinton Broth, Mueller Hinton Agar and Sabouraud Dextrose Agar, Folin–Ciocalteu reagent, sodium carbonate, and Gallic acid with the highest purity available were purchased from Merck (Darmstadt, Germany). Ammonia solution (25% w/w) was provided from chem. Lab Company. Double-distilled water was used for further dilution throughout the study.

UV–vis spectral analysis of CuS nanoparticles and optical absorption measurements of the particles were carried out on a Perkin Elmer Lambda 25 spectrophotometer at room temperature in the wavelength range 300–800 nm. The band gap energy value was estimated from the UV–visible spectroscopic data. The surface textural and morphological properties of the nanoparticles were investigated by field emission scanning electron microscopy (FE-SEM: Hitachi S-4160) under an acceleration voltage of 30 kV. For FE-SEM, it is necessary to coat the nanoparticles with gold, which was carried out by an Auto Fine Coater (JFC-1300, JEOL).

The morphology and particle size distribution of the nanoparticles were determined using a transmission electron microscopy (TEM jeol 300 kV); the TEM images show that the synthesized CuS nanoparticles were within the size of about 10–20 nm. Further, X-ray diffraction (XRD) analysis has been carried out to confirm the crystallinity of the synthesized CuS nanoparticles. XRD pattern was recorded by an automated Philips X'Pert X-ray diffractometer with Cu–Kα radiation (40 kV and 30 mA) for 2θ values over 30°–75° (for CuS-NPs).

2.2. Synthesis of copper sulfide nanoparticles

The CuS nanoparticles were synthesized by the reaction of the precursor material, i.e. Copper(II) acetate [$Cu(CH_3COO)_2{\cdot}H_2O$], with thioacetamide [CH_3CSNH_2] in aqueous media. In a typical synthesis procedure, 10 mL of a 0.1 mol L^{-1} [$Cu(CH_3COO)_2{\cdot}H_2O$] and 20-mL 0.2 mol L^{-1} tri-sodium citrate as capping agents were taken in a 100-mL beaker. In the next step, 5 mL of 0.4 mol L^{-1} thioacetamide (TAA) as source for S^{2-} ions was added to it slowly. Finally, double-distilled water was added to the solution to make the volume close to 100 mL and the solution was stirred well for 1 min. The resulting mixture was placed at room temperature and the citrate-stabilized CuS nanoparticles started to grow slowly. Initially, the color of the solution was blue, but after several minutes, it turned green, and then shifted to brown rapidly [41,42].

2.3. Preparation of plant extract

Root and shoot of *L. usitatissimum* were first washed thoroughly to remove impurities, dried, and then grinded in the form of fine powder. To prepare extracts, the powder (10 gm dry weight) was extracted with 50 ml of absolute ethanol/water (80:20) and kept in a shaker for 48 h. The extract was then centrifuged for 20 min and the supernatant was collected. Solvent was removed with the help of a rotary evaporator and stored at −20°C.

2.4. Antimicrobial bioassay procedure

Well diffusion and broth macrodilution methods were used to elucidate and investigate the antimicrobial activities of the synthesized CuS-NPs. Broth dilution method was performed for antibacterial tests. All the glassware, media, and reagents used in the tests were sterilized in an autoclave at 121˚C, 103 kPa pressures for 21 min prior to the tests. *In vitro* antibacterial and antifungal properties of the root and shoot of *L. usitatissimum* extracts with CuS nanoparticles were tested against Gram-positive (*Staphylococcus aureus*: ATCC 25293) and Gram-negative (*A. Baumannii* ATCC: 150504, *Klebsiella pneumonia*: ATCC 1827, and *Escherichia coli*: ATCC 33218) bacteria and fungi (*Aspergillus oryzae* PTCC 5164). Whatman filter paper no. 1 disks of 6-mm diameter were impregnated with 20-μL CuS-NPs dose (prepared in dimethyl sulfoxide) of 20-mg/mL concentration. The disks were incubated at 37˚C for 24 h and then impregnated on petri plates, with pre-grown microbial culture in it.

2.4.1. Antimicrobial screening using broth dilution method

Broth dilution method was performed to screen the antibacterial activity of the developed mixture. The process was carried out as follows: serial dilution of extracts was performed and nanoparticles in DMSO were used as solvent to obtain a series of concentrations; later, Muller Hinton broth was used as the basal media and the bacteria were incubated at 37˚C for 24 h. Minimum inhibitory concentration (MIC) and minimum bactericidal concentration (MBC) values of extracts and nanoparticles against the bacterial strains were determined according to the method reported elsewhere [43]. The MIC of the compounds was calculated against a specified bacterium based on a broth dilution method. In this method, series of concentrations of extracts and nanoparticles (CuS-NP's) were prepared in sterile test tubes using serial dilution method. Then, 0.65 mL of sterile Muller Hinton broth medium was added to 0.1 mL of bacterium culture test tubes and the test tubes were incubated at 37˚C for 24 h. MIC is determined as the lowest concentration of antibacterial agent that inhibits the visible growth of or reduces the number of colonies of the micro-organism. MBC of CuS-NPs was investigated according to the method reported elsewhere [23]. MBC is determined as the lowest concentration of antimicrobial agent that kills all the test micro-organism, with complete absence of microbial growth (Table 1).

Table 1
Review of sensitivity of bacteria by broth dilution method (MIC and MBC)

Bacteria	CuS-Shoot of *L. usitatissimum*		CuS-Root of *L. usitatissimum*	
	MIC[b]	MBC[b]	MIC[a]	MBC[a]
Klebsiella pneumonia	1.16	4.65	2.38	9.54
Acinetobacter baumannii	0.14	2.33	74.50[b]	0.15
Escherichia coli	9.31	18.62	9.54	19.08
Staphylococcus aureus	0.29	4.650	1.2	2.38

[a]Concentrations (ng/ml).
[b]Concentrations (pg/ml).

2.4.2. Antimicrobial screening using disk diffusion method

Antibacterial activity of CuS-NPs was also tested by agar disk diffusion method reported elsewhere [44]. Hundred microliters of fresh bacterial culture was gently spread on the agar surface [43]. The bacterial concentration utilized was of 5×10^5 CFU/ml. Filter paper disks of 6-mm diameter, impregnated with 20-μL dose of CuS-NPs with concentration 20 mg/mL, were used for screening antibacterial activities against *K. pneumonia*, *A. Baumannii*, *E. coli*, and *S. aureus* grown on culture plates. Culture plates were incubated at 37˚C for 24 h. After incubation, inhibition zone of bacterial growth was measured in mm. *Gentamicin* and *Cephalexin* (10 μg per 100 μl) were used as controlled antibacterial agents, Table 2.

2.4.3. Antifungal screening using disk diffusion method

A. oryzae (PTCC 5164) was used for investigating the antifungal activities of the extract with CuS nanoparticles by the disk diffusion method on the surface of Sabouraud Dextrose Agar inoculated with 10^5 (CFU/mL) of spore suspension of fungi. The petri dishes of *A. oryzae* medium were incubated at 30˚C for 24–48 h. The disks impregnated in extract/nanoparticles solution (containing 20 μL of 600 μg/mL μg of extracts and CuS nanoparticles (1:1) in 5% DMSO) were put at different positions on the agar surface [43]. Finally, antifungal activities of the compounds were evaluated as diameter of inhibition zone from the fungal strains' growth. Antifungal activities of standard drug including *Amphotericin B* (10 μg per 100 μl) have been presented in Table 3.

Table 2
Antibacterial activity as diameter of zone of inhibition[a] (mm) around the constructed disks

Bacteria	CuS-Shoot of *L. usitatissimum*	CuS-Root of *L. usitatissimum*	Cephalexin	*Gentamicin*
Klebsiella pneumonia	12.06	13.20	9.13	9.44
Acinetobacter baumannii	17.56	23.60	10.00	11.80
Escherichia coli	12.46	13.08	–[b]	10.00
Staphylococcus aureus	12.04	11.70	12.00	10.11

[a]All data are the mean of three measurements.
[b]No zone of inhibition.

Table 3
Antifungal activity as diameter of zone of inhibition[a] (mm) around the constructed disks

Compound (mg/disk)	*Aspergillus oryzae*
Root of *L. usitatissimum*/CuS	11.96
Shoot of *L. usitatissimum*/CuS	11.57
Amphotericin B	11.00

[a]All data are the mean of three measurements.

2.5. Determination of the total phenolic content

The total phenolic content (TPC) of the *L. usitatissimum* extracts was determined using Folin–Ciocalteu reagent [45]. Hundred microliters of the diluted ethanolic extracts containing 500-μg extract was mixed separately with (500 μl) Folin–Ciocalteu reagent and diluted with distilled water and 0.4 ml of (7.5% w/v) sodium carbonate solution (Na_2CO_3). The solution was mixed and allowed to stand for 1 h at room temperature. Gallic acid solution (from 25 to 300 μg/ml) was used as a standard reagent. Finally, the absorbance was measured at 765 nm using a UV–vis spectrophotometer. A calibration curve was prepared using standard solutions of gallic acid. The results were expressed as mg gallic acid equivalents (GAE)/g of the dried extract.

2.6. Determination of total flavonoid

Total flavonoid content of extracts was also determined [46]. One milligram of extracts was diluted with 1,000 μl of distilled water and 100 μl of 5% NaNO2 solution was added. The mixture was kept at room temperature for 5 min and then 200 μl of 10% $AlCl_3$ was added to it. This mixture was incubated at room temperature for 6 min then 1 ml of 1 M NaOH was added to the mixture. The solution absorbance at 510 nm was measured with a UV–vis spectrophotometer. The concentration of the flavonoid compounds was calculated using the equation that was obtained from the rutin (50–500 μg/ml) calibration curve.

2.7. Scavenging effect on 2,2-diphenyl-1-picrylhydrazyl

Free radical scavenging activity was estimated by 2,2-diphenyl-1-picryl-hydrazyl (DPPH) assay using von Gadow method with some modifications [47]. 2.4 ml of DPPH radical solution (24 μg/ml) was prepared in 70% aqueous ethanol. The reaction mixture contained 100 μl of test extracts and 1 ml of methanolic solution of (24 μg/ml) of DPPH radical. The mixture was then shaken vigorously and incubated at 37˚C for 10 min. The absorbance was measured at 517 nm using trolex solutions (100–1,000 μg/ml) as a standard. Lower absorbance of the reaction mixture indicated higher free radical scavenging activity which was calculated using the following equation: DPPH scavenging effects (%) = 100 × (Ac–As)/(Ac), where Ac is the absorbance of the control reaction and As is the absorbance of reaction mixture containing DPPH and extract at 517 nm.

2.8. Ferric reducing antioxidant power

Freshly prepared Ferric reducing antioxidant power (FRAP) reagent contained 5 mL of a 10 mM TPTZ (2,4,6-tripyridyl-2-triazine) solution in 40 mM HCl; 5 mL of 20 mM $FeCl_3{\cdot}6H_2O$; and 50 ml of 300 mM acetate buffer (pH 3.6) and was heated at 37˚C. Hundred microliters of various extracts (10 mg/ml) was mixed with 900 μl of FRAP reagent and the mixture was then incubated at 37˚C for 6 min. FRAP of the extracts was determined by modified Benzie and Strain method [48]. The absorbance of the colored reaction mixture (ferrous tripyridyltriazine complex) was measured at 595 nm using standard trolox (1 mg/ml) to estimate the percentage of iron reduced. The standard curve was constructed using iron(II) sulfate solution, and the results were expressed as μmol Fe(II)/mg of dried extract.

2.9. FT-IR Spectrum analysis of Linum usitatissimum

FT-IR (JASCO FT/IR-460 System in the 400–4,000 cm^{-1}, Japan) relies on the fact that most

molecules absorb light in the infrared region of the electromagnetic spectrum. This absorption corresponds specifically to the bonds present in the molecule. The frequency ranges are measured as wave numbers typically over the range 4,000–400 cm^{-1}. Fig. 1 shows the FT-IR peaks of dried *L. usitatissimum* extract; the presence of hydroxyl group in alcoholic and phenolic compounds was supported by the presence of a strong peak at approximately 3,397.96 cm^{-1}. The absorbance bands at 2,933, 1,621, 1,402, 1,265, 1,058, and 595 cm^{-1} are associated with the stretch vibrations of alkyl C–C, conjugated C–C with a benzene ring, bending in plate of C–O–H, C–O stretch, and bending out of plate C–H in saturated tertiary or secondary highly symmetric alcohol in *L. usitatissimum* extract, respectively.

3. Results and discussion

3.1. XRD, SEM, and TEM analyses

Absorption spectra measurements were extended to much longer times than the 30 min shown in (Fig. 2(A)); the CuS nanoparticles' suspension shows a well-resolved absorption maximum of the first electronic transition indicating a sufficiently narrow size distribution of the CuS nanoparticles, which shifts to shorter wavelengths with decreasing size of the nanoparticles as a consequence of quantum confinement. As Fig. 2 exhibits, the citrate-capped CuS nanoparticles have absorption edges in the range 390–416 nm. From the absorption spectra, energy band gap (E_g) of CuS nanoparticles was obtained using the following relation (Fig. 2(B)) [49]:

$$(\alpha h\upsilon) = A(E_g - h\upsilon)^{n/2} \quad (1)$$

where $h\upsilon$ is the incident photon energy, A is a constant, and the exponent n depends on the type of transition, $n = 1$ and 4 for direct and indirect transitions, respectively. As we know, semiconductors such as CuS are considered as direct band gap semiconductors. A typical graph of $(\alpha h\upsilon)^2$ vs. energy ($h\upsilon$) for CuS nanoparticles synthesized at different times is plotted. The band gap energy is obtained by extrapolating the linear portion of $(\alpha h\upsilon)^2$ vs. $h\upsilon$ plot to the energy axis at $\alpha = 0$. The straight-line characteristic of the curve indicated that the CuS nanoparticles have direct band gap in the range 2.98–3.17 eV, while the bulk material has a band of 2.2 eV [50]. This increase in E_g of the CuS nanoparticles can be assigned to the quantum size effect as expected from the nanocrystalline nature of the CuS nanoparticles [51].

Fig. 3 reveals the XRD pattern obtained by scanning 2θ for the powder of CuS nanoparticles prepared at room temperature. It exhibits seven major diffraction peaks related to the diffraction angles 32.33° (1 0 1), 34.25° (1 0 2), 37.13° (1 0 3), 38.20° (0 0 6), 56.37° (1 1 0), 62.23° (1 0 8), and 70.20° (1 1 6). This pattern confirmed the formation of a hexagonal covellite phase (CuS), which has good agreement with the standard XRD pattern (Joint Committee for Powder

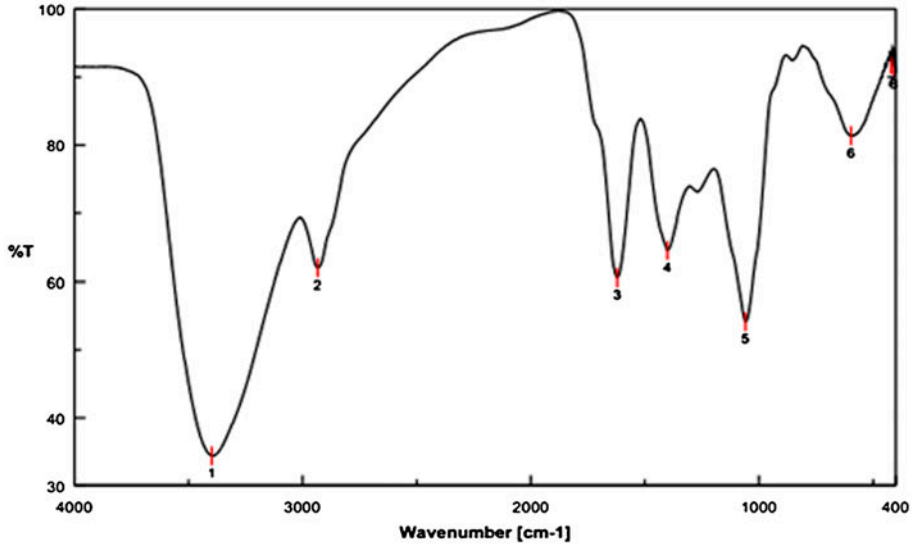

Fig. 1. Fourier transform infrared absorption spectra of dried *L. usitatissimum* extract.

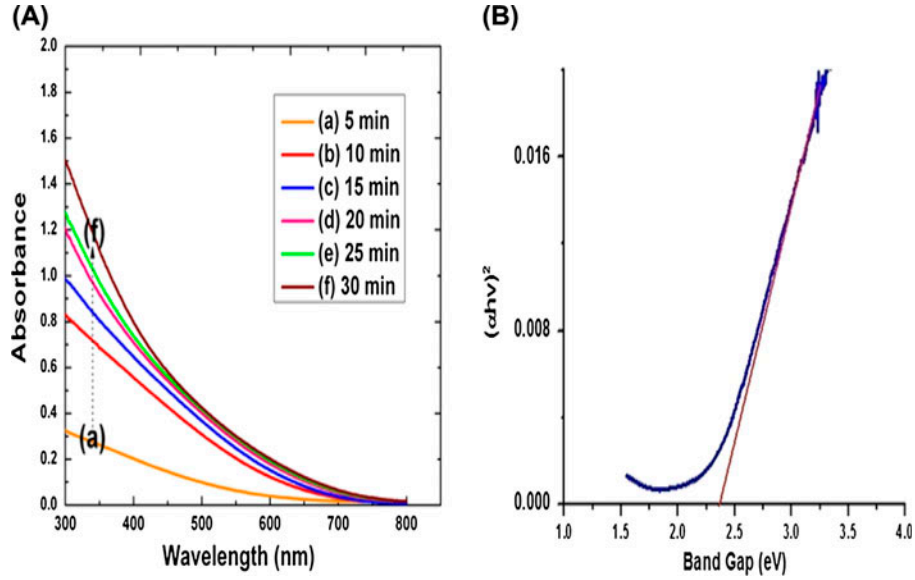

Fig. 2. (A) Evolution of absorption spectra of the CuS nanoparticles taken at 5-min intervals following the initiation of the reaction for the first 30 min and (B) the plot of $(\alpha h\nu)^2$ vs. band gap (eV).

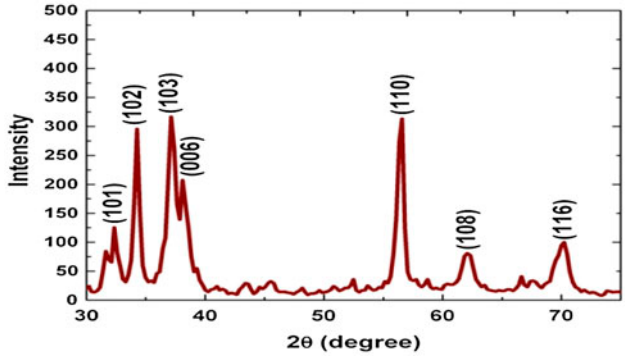

Fig. 3. XRD pattern of the CuS nanoparticles.

Diffraction Standards, JCPDS card No. 24-0060) [52]. The average nanocrystallite's size (D) is estimated according to the Debye–Scherer equation [53]:

$$D = \frac{K\lambda}{\beta \cos\theta} \quad (2)$$

The surface morphology and textural properties of the prepared CuS nanoparticles were investigated by FE-SEM (Fig. 4(A)). Morphology and size of the prepared CuS nanoparticles were also investigated by TEM technique. The TEM images of CuS are shown in (Fig. 4(B)). In TEM images, the rod nanoparticles were about 20 nm.

3.2. Antimicrobial bioassays (in vitro)

The compounds were tested against Gram-positive (*S. aureus:* ATCC 25293) and Gram-negative (*A. Baumannii*: ATCC150504, *K. pneumonia*: ATCC1827, and *E. coli*: ATCC 33218) bacteria. The antibacterial activities with agar diffusion method data of the compounds have been compiled in (Table 2). In *L. usitatissimum*, shoot extract loaded with CuS nanoparticles exhibited higher antibacterial activities against all bacterial strains. Obtained results revealed that the shoot extract possess more effective antibacterial properties in comparison with the root extract loaded with CuS nanoparticles; while in case of antifungal properties, obtained results revealed that the root extract loaded with CuS nanoparticles possess more effective antifungal properties in comparison with the shoot extract loaded with CuS nanoparticles. The image of inhibition zones around constructed disks and MBC are shown in (Fig. 5). Antibacterial effects of metallic nanoparticles are stronger than other nanomaterials, which exhibit increasing chemical activity due to their large surface to volume ratios and crystallographic surface structure. Using medicinal plant extracts with metal nanoparticles can be effective to eliminate bacterial infections, as an alternative to antibiotics. The antifungal activities of CuS-NPs as zone diameter of inhibition (mm) from the growth were tested against *A. oryzae* as fungal strains according to the defined method [54]. Antifungal activities of the constructed disks showed considerable difference for compounds

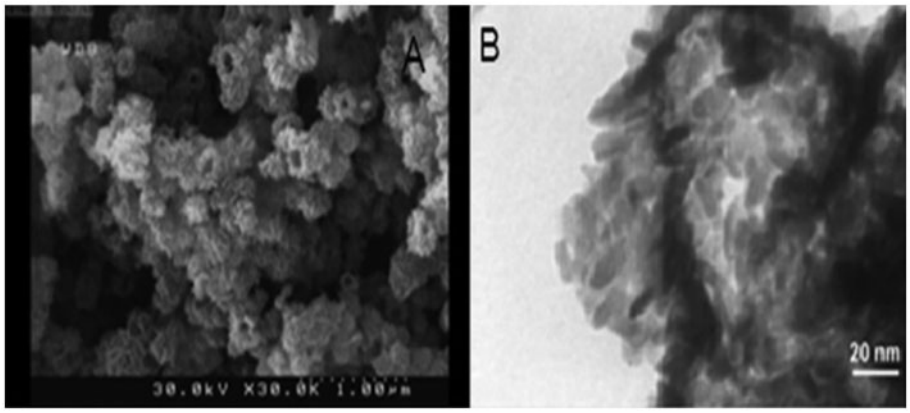

Fig. 4. FE-SEM (A) and TEM and (B) images of CuS nanoparticles.

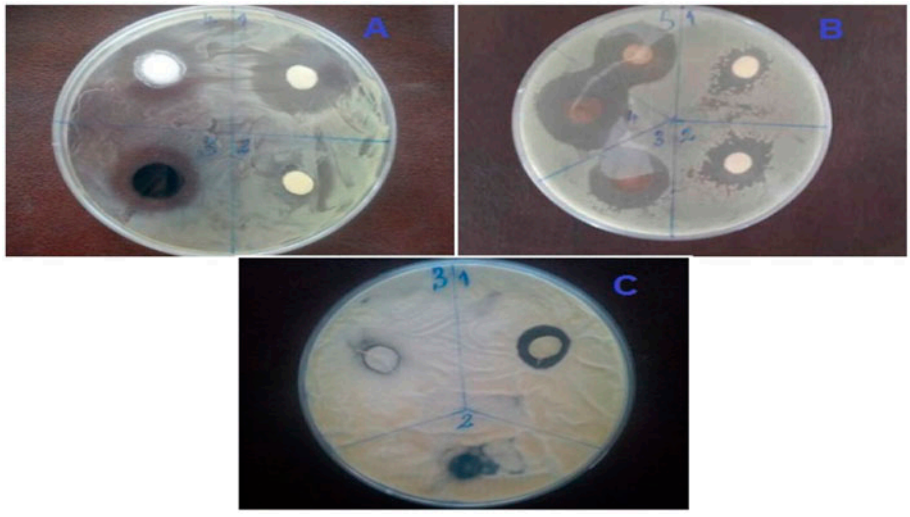

Fig. 5. Some images of inhibition zones around constructed disks on agar plates. (A and B) Root extract/CuS and shoot extract/CuS against *A. baumannii* and *Staphylococcus aureus*, (C) Root extract/CuS and shoot extract/CuS against *A. oryzae*, respectively.

(Table 3). Shoot extract of *L. usitatissimum*/CuS was more effective than root.

3.3. Total flavonoid and phenolic contents

Flavonoids are polyphenolic compounds which play an important role in stabilizing lipid oxidation are also associated with anti-oxidative action [55]. Flavonoids found ubiquitously in plants are the most common group of phytophenolics. Flavonoid content of the extracts in terms of (mg/g) rutin equivalents was recorded.

Phenols are the simplest bioactive photochemicals, which posses the ability to act as free radical scavengers due to the presence of hydroxyl groups (–OH). The active sites and the number of hydroxyl groups are directly related to their relative toxicity for the micro-organisms and recently it was discovered that the increase in the hydroxyl groups or hydroxylation sites leads to the increase in the toxicity properties of these compounds [56]. The phenolic contents of hydroalcoholic extracts of plants were tested using the diluted Folin–Ciocalteu reagent (FCR). Phenolic compounds react with FCR only under basic conditions (adjusted by a sodium carbonate solution to pH 10). Dissociation of a phenolic proton leads to a phenolate anion, which is capable of reducing FCR. The reaction occurs through electron transfer mechanism. The blue compounds formed between phenolate and FCR are independent of the structure of phenolic compounds,

Table 4
Total phenolic and flavonoid content and antioxidant activity of hydroalcoholic extracts

Extracts	TPC[a]	TF[b]	(DPPH) inhibition %	FRAP[c]
Root of *L. usitatissimum*	85.73 ± 0.66	51.1 ± 0.37	19.17 ± 0.57	546.3 ± 2.23
Shoot of *L. usitatissimum*	128.24 ± 1.127	95.04 ± 0.53	30.57 ± 0.4	957.8 ± 3.81

[a]TPC: total phenolic content, mg gallic acid equivalent/g of dried extract
[b]TF: total flavonoid content, mg rutin equivalents (RuE)/g of dried extract.
[c]FRP: ferric reducing power content, μmol Fe(II)/mg of dried extract.

therefore ruling out the possibility of coordination complexes formed between the metal center and the phenolic compounds. It is believed that FCR contains hetero polyphosphotunstates molybdates [57]. The highest contents of total flavonoids and phenols were observed in the shoot of *L. usitatissimum* (Table 4 and Fig. 6).

3.4. Antioxidant capacity

Recently, the use of antioxidants is proposed to protect people from oxidative stress damages. This study indicated that higher concentration of phenolic compounds in hydroalcoholic extracts improved antioxidant activity. These plants can be used as a source of natural antioxidants to remove harmful effects of free radicals. The *in vitro* antioxidant activity of test extracts was estimated using DPPH and FRAP assays. DPPH radical scavenging activity test measures the capacity of the extracts to scavenge the stable radical 2,2-diphenyl-1-picrylhydrazyl. If the extracts have this capacity, the initial blue/purple solution will change to a yellow color due to the formation of diphenyl picryl hydrazine. The antioxidants reacted with DPPH, a purple-colored stable free radical, which accepts an electron or hydrogen radical to become a stable diamagnetic molecule. The amount of DPPH reduced was estimated by measuring the decrease in absorbance at 517 nm [57]. The highest DPPH radical scavenging and ferric reducing power (FRP) was obtained by aqueous/ethanolic extract of *L. usitatissimum* shoot (Bois leaves 30.57 ± 0.69% and 957.330 ± 3.81) (Fig. 7) and results are presented in Table 4. FRAP, on the other hand, gives a direct measure of antioxidants or reductants in a sample which react with ferric tripyridyltriazine (Fe^{3+} TPTZ) complex and produce a colored product, ferrous tripyridyltriazine (Fe^{2+} TPTZ) [57]. FRAP assay is a simple assay that gives fast and reproducible results. In this assay, antioxidants in test samples reduced the ferricyanide complex to the ferrous form by donating an electron. Fe^{3+} reduction is often used as an indicator of electron-donating activity, which is an important mechanism of

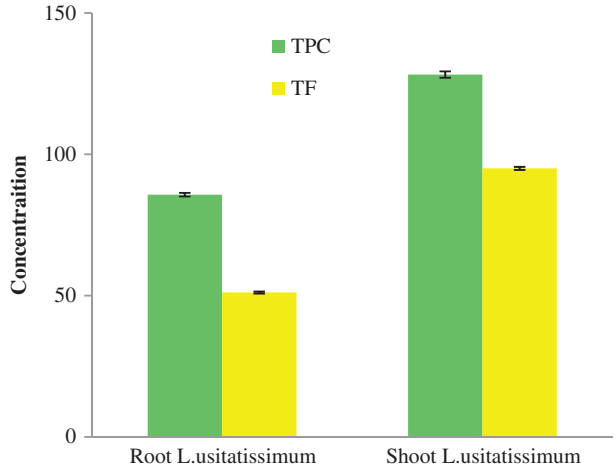

Fig. 6. Total flavonoids and total pheonlic content present in root and shoot extract of *L. usitatissimum* (TPC: mg gallic acid equivalent/g of dried extract and TF: mg rutin equivalents (RuE)/g of dried extract).

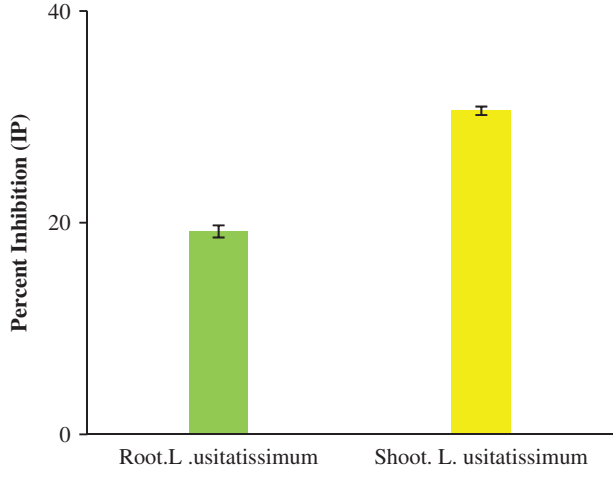

Fig. 7. Comparison of inhibition percent.

phenolic antioxidant action. *L. usitatissimum* plant powder showed the characteristic fluorescence when treated with different reagents which supported results of phytochemical studies. Preliminary phytochemical

Table 5
Infrared spectrum analysis of *L. usitatissimum*

S. no.	Peak value	Stretching	Interpretation
1	420.40	C–H bending outside of page	Alkanes
2	595.89	C–O stretching	Alcohols
3	1,060.66	O–H bending outside of page	Alcohols
4	1,402.00	C–H bending	Alkanes
5	1,621.84	C=C stretching	Alkenes
6	2,933.20	C–H stretching	Alkanes
7	3,397.96	O–H stretching	Alcohols

investigations in plant *L. usitatissimum* powder showed the presence of flavonoids, tannins, sterols, phenolic compounds, and saponins (Table 5). The different types of functional groups of *L. usitatissimum* extract are identified in Fig. 7 and Table 5.

4. Conclusions

In the present study, the antibacterial and antifungal properties of CuS nanoparticles combined with root and shoot extracts from *L. usitatissimum* were screened against one type of Gram-positive and three Gram-negative bacteria: *S. aureus*, *A. Baumannii*, and *A. oryzae* fungal, using agar well diffusion method and comparing their antibacterial activities with the antibiotics *Gentamicin*, *Cephalexin*, and *Amphotericin B*. Information of MIC and MBC of both samples showed that biological CuS nanoparticles have more antibacterial and antifungal effects than CuS nanoparticles. Therefore, by completion of these experiments, the use of metal nanoparticles with plant extracts in sensitive environments, such as hospital, is suggested. Among the most promising nanomaterials with antibacterial properties are metallic nanoparticles, which exhibit increasing chemical activity due to their large surface to volume ratios and crystallographic surface structure. Using medicinal plant extracts with metal nanoparticles can be effective in eliminating bacterial infections, as an alternative to antibiotics. *L. usitatissimum* is an abundant source of lignins, which have antioxidant properties and significantly reduce the effects of free radicals. The antioxidant content of the extracts was also determined and demonstrated the highest antioxidant activities associated with the shoot of *L. usitatissimum* (TPC 1: 128.24 ± 1.127-mg gallic acid equivalents/g of dried extract, DPPH: 30.57 ± 0.4% inhibition, FRAP: 957.8 ± 3.81 μmol Fe(II)/mg of dried extract, and Total Flavonoid Content: 2: 95.04 ± 0.53-mg rutin equivalents (RuE)/g of dried extract). The CuS-NPs showed strong activity against all micro-organisms tested.

Acknowledgments

This work was supported by a grant from Research Council of Yasouj University.

References

[1] R. Premanath, N. Lakshmideri, Studies on antioxidant activity of *Tinospora cordifolia* (Miers) leaves using *in vitro* models, J. Am. Sci. 6 (2010) 736–743.
[2] J. Owolabi, E.K.I. Omogbai, O. Obasuyi, Antifungal and antibacterial activities of the ethanolic and aqueous extract of *Kigella africana* (*Bignoniaceae*) stem bark, Afr. J. Biotechnol. 6 (2007) 882–885.
[3] J. Cheon, G. Horace, Inorganic nanoparticles for biological sensing, imaging and therapeutics, J. Mater. Chem. 19 (2009) 6249–6250.
[4] S. Baker, S. Satish, Endophytes: Toward a vision in synthesis of nanoparticles for future therapeutic agents, J. Bio-Inorg. Hybd. Nanomat. 1 (2012) 1–11.
[5] E. Bae, H.J. Park, J. Lee, Y. Kim, J. Yoon, K. Park, Bacterial cytotoxicity of the silver nanoparticle related to physicochemical metrics and agglomeration properties, Environ. Toxicol. Chem. 29 (2010) 2154–2160.
[6] S. Gurunathan, K. Kalishwaralal, R. Vaidyanathan, D. Venkataraman, S.R. Pandian, J. Muniyandi, Biosynthesis, purification and characterization of silver nanoparticles using *Escherichia coli*, Colloids Surf. B: Biointerfaces 74 (2009) 328–335.
[7] S. Pal, Y.K. Tak, J.M. Song, Does the antibacterial activity of silver nanoparticles depend on the shape of the nanoparticle? A study of the gram-negative bacterium *Escherichia coli*, Appl. Environ. Microbiol. 73 (2007) 1712–1720.
[8] P. Evans, H. Matsunaga, M. Kiguchi, Large-scale application of nanotechnology for wood protection, Nat. Nanotechnol. 3 (2008) 577–577.
[9] Y. Wu, C. Wadia, W. Ma, B. Sadtler, A.P. Alivisatos, Synthesis and photovoltaic application of copper(I) sulfide nanocrystals, Nano Lett. 8 (2008) 2551–2555.
[10] L. Youngil, C. Jun-rak, L. Kwi Jong, E.S. Nathan, K. Donghoon, Large-scale synthesis of copper nanoparticles by chemically controlled reduction for applications of inkjet-printed electronics, Nanotechnology 19 (2008) 415–604.
[11] G. Ren, D. Hu, E.W.C. Cheng, M.A. Vargas-Reus, P. Reip, R.P. Allaker, Characterisation of copper oxide nanoparticles for antimicrobial applications, Int. J. Antimicrob. Agents 33 (2009) 587–590.

[12] A. Pandey, S. Brovelli, R. Viswanatha, L. Li, J.M. Pietryga, V.I. Klimov, S.A. Crooker, Long-lived photoinduced magnetization in copper-doped ZnSe-CdSe core-shell nanocrystals, Nat. Nanotechnol. 7 (2012) 792–797.
[13] R.A. Maithreepala, R. Doong, Reductive dechlorination of carbon tetrachloride in aqueous solutions containing ferrous and copper ions, Environ. Sci. Technol. 38 (2004) 6676–6684.
[14] M.H. Dehghani, M.M. Taher, A.K. Bajpai, B. Heibati, I. Tyagi, M. Asif, S. Agarwal, V.K. Gupta, Removal of noxious Cr (VI) ions using single-walled carbon nanotubes and multi-walled carbon nanotubes, Chem. Eng. J. 279 (2015) 344–352.
[15] I. Perelshtein, G. Applerot, N. Perkas, E. Wehrschuetz-Sigl, A. Hasmann, G. Guebitz, A. Gedanken, CuO–cotton nanocomposite: Formation, morphology, and antibacterial activity, Surf. Coat. Technol. 204 (2009) 54–57.
[16] Y. Li, W. Lu, Q. Huang, M. Huang, C. Li, W. Chen, Copper sulfide nanoparticles for photothermal ablation of tumor cells, Nanomedicine 5 (2010) 1161–1171.
[17] X. Yanping, H. Yiping, P.L. Irwin, J. Tony, S. Xianming, Antibacterial activity and mechanism of action of zinc oxide nanoparticles against *Campylobacter jejuni*, Appl. Environ. Microbiol. 77 (2011) 2325–2331.
[18] H. Sadegh, R. Shahryari-ghoshekandi, S. Agarwal, I. Tyagi, M. Asif, V.K. Gupta, Microwave-assisted removal of malachite green by carboxylate functionalized multi-walled carbon nanotubes: Kinetics and equilibrium study, J. Mol. Liquids 206 (2015) 151–158.
[19] S. Nagarajan, K.A. Kuppusamy, Extracellular synthesis of zinc oxide nanoparticle using seaweeds of gulf of Mannar, India, J. Nanobiotechnol. 11 (2013) 39–50.
[20] R.J.B. Pinto, S. Daina, P. Sadocco, C.P. Neto, T. Trindade, Antibacterial activity of nanocomposites of copper and cellulose, Biomed. Res. Int. 280 (2013) 512–518.
[21] N. Tran, A. Mir, D. Mallik, A. Sinha, S. Nayar, T.J. Webster, Bactericidal effect of iron oxide nanoparticles on *Staphylococcus aureus*, Int. J. Nanomed. 5 (2010) 277–283.
[22] V.K. Gupta, I. Ali, Removal of DDD and DDE from wastewater using bagasse fly ash, a sugar industry waste, Water Res. 35 (2001) 33–40.
[23] V.K. Gupta, S. Sharma, I.S. Yadav, D. Mohan, Utilization of Bagasse fly ash generated in sugar industry for the removal and recovery of phenol and p-nitrophenol from wastewater, J. Chem. Technol. Biotechnol. 71 (1998) 180–186.
[24] V.K. Gupta, A. Mittal, D. Jhare, J. Mittal, Batch and bulk removal of hazardous colouring agent Rose Bengal by adsorption techniques using bottom ash as adsorbent, RSC Adv. 2 (2012) 8381–8389.
[25] V.K. Gupta, I. Ali, V.K. Saini, T. Van Gerven, B. Van der Bruggen, C. Vandecasteele, Removal of dyes from wastewater using bottom ash, Ind. Eng. Chem. Res. 44 (2005) 3655–3664.
[26] T.A. Saleh, S. Agarwal, V.K. Gupta, Synthesis of MWCNT/MnO_2 composites and their application for simultaneous oxidation of arsenite and sorption of arsenate, Appl. Catal. B: Environ. 106 (2011) 46–53.
[27] H. Khani, M.K. Rofouei, P. Arab, V.K. Gupta, Z. Vafaei, Multi-walled carbon nanotubes-ionic liquid-carbon paste electrode as a super selectivity sensor: Application to potentiometric monitoring of mercury ion(II), J. Hazard. Mater. 183 (2010) 402–409.
[28] V.K. Gupta, R. Kumar, A. Nayak, T.A. Saleh, M.A. Barakat, Adsorptive removal of dyes from aqueous solution onto carbon nanotubes: A review, Adv. Colloid Interface Sci. 193–194 (2013) 24–34.
[29] T.A. Saleh, V.K. Gupta, Photo-catalyzed degradation of hazardous dye methyl orange by use of a composite catalyst consisting of multi-walled carbon nanotubes and titanium dioxide, J. Colloid Interface Sci. 371 (2012) 101–106.
[30] V.K. Gupta, S.K. Srivastava, D. Mohan, S. Sharma, Design parameters for fixed bed reactors of activated carbon developed from fertilizer waste for the removal of some heavy metal ions, Waste Manage. 17 (1998) 517–522.
[31] V.K. Gupta, P. Singh, N. Rahman, Adsorption behavior of Hg(II), Pb(II), and Cd(II) from aqueous solution on Duolite C-433: A synthetic resin, J. Colloid Interface Sci. 275 (2004) 398–402.
[32] S. Karthikeyan, V.K. Gupta, R. Boopathy, A. Titus, G. Sekaran, A new approach for the degradation of high concentration of aromatic amine by heterocatalytic Fenton oxidation: Kinetic and spectroscopic studies, J. Mol. Liquids 173 (2012) 153–163.
[33] V.K. Gupta, R. Jain, A. Nayak, S. Agarwal, M. Shrivastava, S. Agarwal, S. Sikarwar, Removal of the hazardous dye—Tartrazine by photodegradation on titanium dioxide surface, Mater. Sci. Eng. C 31 (2011) 1062–1067.
[34] V.K. Gupta, A. Nayak, Cadmium removal and recovery from aqueous solutions by novel adsorbents prepared from orange peel and Fe_2O_3 nanoparticles, Chem. Eng. J. 180 (2012) 81–90.
[35] V.K. Gupta, B. Gupta, A. Rastogi, S. Agarwal, A. Nayak, Pesticides removal from waste water by activated carbon prepared from waste rubber tire, Water Res. 45 (2011) 4047–4055.
[36] V.K. Gupta, A. Nayak, S. Agarwal, I. Tyagi, Potential of activated carbon from waste rubber tire for the adsorption of phenolics: Effect of pre-treatment conditions, J. Colloid Interface Sci. 417 (2014) 420–430.
[37] V.K. Gupta, A.K. Jain, G. Maheshwari, Aluminum(III) selective potentiometric sensor based on morin in poly (vinyl chloride) matrix, Talanta 72(4) (2007) 1469–1473.
[38] V.K. Gupta, M.R. Ganjali, P. Norouzi, H. Khani, A. Nayak, Shilpi Agarwal, Electrochemical analysis of some toxic metals by ion–selective electrodes, Crit. Rev. Anal. Chem. 41 (2011) 282–313.
[39] V.K. Gupta, A.K. Jain, S. Agarwal, G. Maheshwari, An iron(III) ion-selective sensor based on a μ-bis(tridentate) ligand, Talanta 71 (2007) 1964–1968.
[40] R.N. Goyal, V.K. Gupta, S. Chatterjee, Voltammetric biosensors for the determination of paracetamol at carbon nanotube modified pyrolytic graphite electrode, Sens. Actuators, B: Chem. 149 (2010) 252–258.
[41] M. Ghaedi, S. Khodadoust, H. Sadeghi, M.A. Khodadoust, R. Armand, A. Fatehi, Application of ultrasonic radiation for simultaneous removal of auramine O and safranine O by copper sulfide nanoparticles: Experimental design, Spectrochim. Acta Part A: Mol. Biomol. Spectrosc. 136 (2015) 1069–1075.

[42] Z.H. Chohan, S.H. Sumrra, M.H. Youssoufi, T.B. Hadda, Metal based biologically active compounds: Design, synthesis, and antibacterial/antifungal/cytotoxic properties of triazole-derived Schiff bases and their oxovanadium(IV) complexes, Eur. J. Med. Chem. 45 (2010) 2739–2747.
[43] A.W. Bauer, W.M.M. Kirby, J.C. Sherris, M. Turck, Antibiotic susceptibility testing by a standardized single disk method, Am. J. Clin. Pathol. 45 (1966) 493–496.
[44] S. McDonald, P.D. Prenzler, M. Antolovich, K. Robards, Phenolic content and antioxidant activity of olive extracts, Food Chem. 73 (2001) 73–84.
[45] J. Zhishen, T. Mengcheng, W. Jianming, The determination of flavonoid contents in mulberry and their scavenging effects on superoxide radicals, Food Chem. 64 (1999) 555–559.
[46] A. von Gadow, E. Joubert, C.F. Hansmann, Comparison of the antioxidant activity of aspalathin with that of other plant phenols of rooibos tea (*Aspalathus linearis*), alpha- tocopherol, BHT, and BHA, J. Agric. Food Chem. 45 (1997) 632–638.
[47] Y. Li, C. Guo, J. Yang, J. Wei, J. Xu, S. Cheng, Evaluation of antioxidant properties of pomegranate peel extract in comparison with pomegranate pulp extract, Food Chem. 96 (2006) 254–260.
[48] R. Sahraei, A. Daneshfar, A. Goudarzi, S. Abbasi, M.H. Majles Ara, F. Rahimi, Optical properties of nanocrystalline ZnS: Mn thin films prepared by chemical bath deposition method, J. Mater. Sci. Mater. Electron. 24 (2013) 260–266.
[49] I. Puspitasari, T.P. Gujar, K.D. Jung, O.S. Joo, Simple chemical preparation of CuS nanowhiskers, Mater. Sci. Eng. B 140 (2007) 199–202.
[50] A.G. Goudarzi, A. Motedayen, S.S. Park, M.C. Choi, R. Sahraei, M. Habib Ullah, A. Avane, C.S. Ha, Low-temperature growth of nanocrystalline mn-doped ZnS thin films prepared by chemical bath deposition and optical properties, Chem. Mater. 21 (2009) 2375–2385.
[51] S.K. Maji, N. Mukherjee, A.K. Dutta, D.N. Srivastava, Deposition of nanocrystalline CuS thin film from a single precursor: Structural, optical and electrical properties, Mater. Chem. Phys. 130 (2011) 392–397.
[52] R. Sahraei, G. Motedayen Aval, A. Goudarzi, Compositional, structural, and optical study of nanocrystalline ZnS thin films prepared by a new chemical bath deposition route, J. Alloys Compd. 466 (2008) 488–492.
[53] N. Dharmaraj, P. Viswanathamurthi, K. Natarajan, Ruthenium (II) complexes containing bidentate Schiff bases and their antifungal activity, Transition Met. Chem. 26 (2001) 105–109.
[54] X. Guoxiu, L. Nan, W. Tong, Y. Meiyan, Advances in studies on flavonoids of Licorice, Zhongguo Zhong Yao Za Zhi. 28 (2003) 593–597.
[55] H. Fujiki, S. Yoshizawa, T. Horiuchi, M. Suganuma, J. Yatsunami, S. Nishiwaki, Anticarcinogenic effects of (-) epigallocatechin gallate, Preventive Med. 21 (1992) 503–509.
[56] D. Huang, B. Ou, R.L. Prior, The Chemistry behind antioxidant capacity assays, J. Agric. Food Chem. 53 (2005) 1841–1856.
[57] T. Yamaguchi, H. Takamura, T. Matoba, J. Terao, HPLC Method for Evaluation of the free radical-scavenging activity of foods by using 1,1-diphenyl-2-picrylhydrazyl, Biosci. Biotechnol. Biochem. 62 (1998) 1201–1204.